Piano soundboard vibro-acoustic modeling through decomposition on the basis of orthotropic simply supported unribbed plate modes

Benjamin Trévisan, Kerem Ege, Bernard Laulagnet

PIANO SOUNDBOARD VIBRO-ACOUSTIC MODELING THROUGH DECOMPOSITION ON THE BASIS OF ORTHOTROPIC SIMPLY SUPPORTED UNRIBBED PLATE MODES

B. Trévisan[1*] , K. Ege[1] and B. Laulagnet[1]

[1]Laboratoire Vibrations Acoustique - INSA de Lyon
Btiment St. Exupéry, 25 bis av. Jean Capelle,
69621 Villeurbanne cedex - France
Email: benjamin.trevisan@insa-lyon.fr

ABSTRACT

The piano soundboard is an orthotropic plate made of spruce, ribbed by multiple stiffeners, with a big additional beam, nearly in a perpendicular direction, the bridge. This complex structure has an essential role in the working of the instrument. Indeed, since strings' sections are too small to radiate by themselves, their vibrations are transmitted to the soundboard which radiates efficiently the sound. The vibro-acoustic models of such a structure are rare and mechanisms involved in piano acoustical radiation are not so easy to undertake. The aim of this study is to concentrate efforts on the modeling of the "radiator": the piano soundboard. In the present paper, focus will be done on the way to calculate the plate soundboard vibration, in the case of special orthotropy, where the ribs and the bridge are present. We develop here a quasi-analytical model of the piano soundboard vibro-acoustical behavior which allows us for example to estimate the sensitivity of rib spacing, or of the bridge on the modal shapes and radiation's indicators as radiated power, space average velocity and soundboard radiation factor through parametric studies.

1 INTRODUCTION

For a long time designed in an empirical manner, musical instruments are now a current subject of study due to perceptive and subjective aspects of the sound produced. Indeed, many parameters influence their colors from woods used [1, 2] to specifications due to conception of the instruments which determine largely their vibratory behavior.
In the case of piano, the soundboard has an essential role in the working of the instrument. Indeed, strings' sections are too thin to radiate by themselves. So their vibrations are transmitted to the

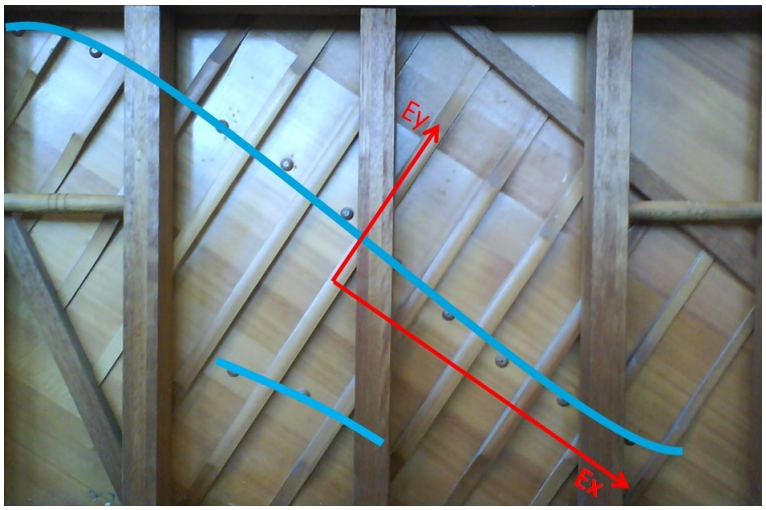

Figure 1. Soundboard of an upright piano.

soundboard through the bridges (in blue in figure 1) which serve as effective acoustic radiator.
This is a structure with a complex geometry constituted by a plate with complex geometry, traditionally made of spruce, pseudo-periodically ribbed on a face by several beams in a direction perpendicular to the fibers of wood, and by one or two bridges on the opposite face in a direction nearly parallel to the fibers. This broadband behavior's structure has been approach several times by Suzuki, Conklin, Giordano [3–5] and more recently by Berthaut, Ege & Boutillon and Chaigne [6–9] and the problematics are leaded by musical questions. Among them, the hunt of a good concession between "sustain / radiated power" or the question of the color of tone not enough rich in high pitched notes seem to be the principal difficulties for piano makers.
Beyond that, this subject has many other industrial applications due to the common using of composite materials and ribbed panels in the conception of structures. Among them : automotive (rear wall of cab's truck), aircraft fuselage or submarine shell. The problem is the same, just change the problematics : boost the radiation in the case of piano or decrease it in the case of transport.
With a view to answering these questions, analysis of the influence of superstructures (ribs) on the vibro-acoustic behavior of an orthotropic ribbed plate is realized by an analytical model based on a variational formulation which permits to quantify the influence of smallest variations of geometry. It's also the possibility to avoid the use of finite element method which is so weighty for several parametric studies in the future.

2 VIBRATORY MODELING

In this study, we are interested in a simplified geometry of an upright piano (see figure 2). We consider a special orthotropic plate (axis of orthoropy parallel to edges in red in 2). Boundary conditions are simply supported and the plate has one straight rib in the direction of the strong Young modulus (one bridge in the direction of the wood's fibers $\vec{x}$) and eleven pseudo-periodic ribs in the perpendicular direction. These superstructures are also made of spruce.
Eccentricity of different superstructures is taken into account. Moreover, thickness of the plate, width and height of superstructures are constant.

The analytical model developed is based on a variational approach drawing its inspiration from Laulagnet & Guyader's works [10, 11]. Moreover, the transversal displacement is developed on the basis of simply supported plate's modes.
We have to calculate kinetic and strain energies of the whole structure to calculate the Hamilton functional of the problem, to develop it on the basis mentioned above in order to write a matrix

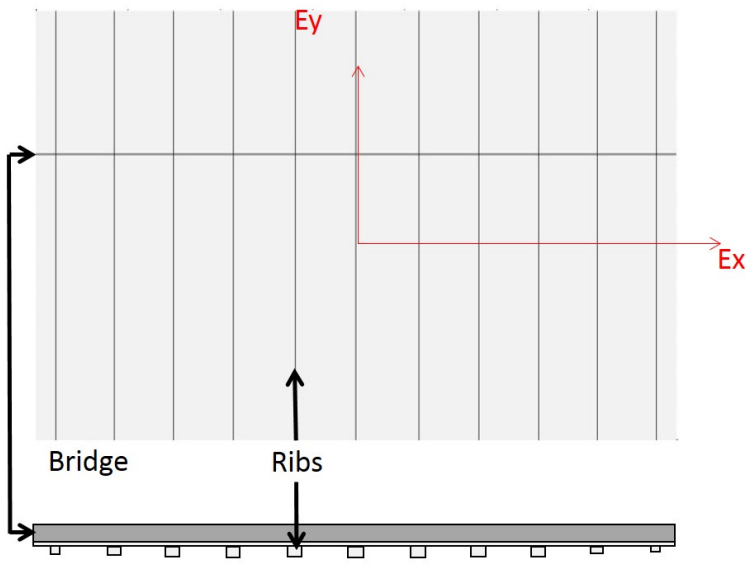

Figure 2: Simplified soundboard of an upright piano used for the analytical modeling. (a) : top view. ; (b) : cross-sectional view of soundboard and ribs (plan (x,z)).

problem and to determine a new specific basis linked to the ribbed structure.

2.1 Kinetic hypothesis

Because the thickness of the soundboard is very small compared to the other dimensions, we adopted the Love-Kirchhoff hypothesis linked to thin plates. So, pumping effects and shearing in the two bending planes are ignored. The middle plane of the plate doesn't admit motion in the direction of plate's edges.
Taking into account these hypothesis and writing the motion as linear into the thickness (limited development at the order 1), it comes the following motion field :

$$\begin{cases} u(x,y,z,t) = -z\,\frac{\partial w}{\partial x} \\ v(x,y,z,t) = -z\,\frac{\partial w}{\partial y} \\ w(x,y,z,t) = w(x,y,t) \end{cases} \tag{1}$$

with $z \in \left[-\frac{h}{2};\frac{h}{2}\right]$ (h being the plate's thickness) and where $u(x,y,z,t)$ and $v(x,y,z,t)$ are the motions in directions $\vec{x}$ and $\vec{y}$ and $w(x,y,t)$ is the plate's transversal displacement.

The different superstructures are considered as beams driven by bending and torsion coupled to the plate. Because only the thin plate perimeter is constrained, supposed simply supported, in the following the thin plate's motion controls the superstructure's motion. Displacements and rotations are considered as continuous at the interface, so we write for a rib in the direction $\vec{y}$ at the position $x = x_r$:

$$\begin{cases} u_r(y,z,t) = -z\,w_{,x}(x_r,y,t) \\ v_r(y,z,t) = -z\,w_{,y}(x_r,y,t) \\ w_r(x,y,t) = w(x_r,y,t) + x\,w_{,x}(x_r,y,t) \end{cases} \tag{2}$$

where $x \in \left[x_r - \frac{b}{2}; x_r + \frac{b}{2}\right]$ and $z \in \left[\frac{h}{2};\frac{h}{2} + H\right]$ and where h and H are respectively thickness of the plate and height of the rib considered and b its width.

2.2 Hamilton functional

From different motion's fields, we express the Hamilton functionals of each sub-parts. These functionals are expressed by the integral of the difference between kinetic and strain energies on an arbitrary time. So, we write successively the actions of the plate, the bending and torsion of a rib in the direction $\vec{y}$ at the position $x = x_r$ and bending and torsion of a bridge in the direction $\vec{x}$ at the position $y = y_c$ by :

$$H_p = \int_{t_0}^{t_1} \frac{1}{2} \int_S \rho h \dot{w}^2 - \left(D_1 w_{,xx}^2 + D_3 w_{,yy}^2 + D_2 w_{,xx} w_{,yy} + D_4 w_{,xy}^2 \right) \, dSdt \tag{3}$$

$$H_{rb} = \int_{t_0}^{t_1} \frac{1}{2} \int_S \left[\rho_r \left(I_f \dot{w}_{,x}^2 + bH\dot{w}^2 \right) - E_r I_f w_{,yy}^2 \right] \delta(x - x_r) \, dSdt \tag{4}$$

$$H_{rt} = \int_{t_0}^{t_1} \frac{1}{2} \int_S \left[\rho_r I_g w_{,x}^2 - G_r I_g w_{,xy}^2 \right] \delta(x - x_r) \, dSdt \tag{5}$$

$$H_{bb} = \int_{t_0}^{t_1} \frac{1}{2} \int_S \left[\rho_c \left(I_{fc} \dot{w}_{,y}^2 + b_c H_c \dot{w}^2 \right) - E_c I_{fc} w_{,xx}^2 \right] \delta(y - y_c) \, dSdt \tag{6}$$

$$H_{bt} = \int_{t_0}^{t_1} \frac{1}{2} \int_S \left[\rho_c I_{gc} w_{,y}^2 - G_c I_{gc} w_{,xy}^2 \right] \delta(y - y_c) \, dSdt \tag{7}$$

where the rib and the bridge are considered as punctual in their widths (justifying the Dirac distributions $\delta(x - x_r)$ and $\delta(y - y_c)$). The following array gives the description of the different constants used in the last equations.

ρ	Plate's mass density	h	Plate's thickness
D_i	Plate's dynamic stiffness	ρ_r	Rib's mass density
E_r	Rib's Young modulus	H	Rib's height
b	Rib's width	I_f	Rib's momentum of bending inertia
G_r	Rib's shear modulus	I_g	Rib's momentum of torsion inertia
E_c	Bridge's Young modulus	H_c	Bridge's height
b_c	Bridge's width	I_{fc}	Bridge's momentum of bending inertia
G_c	Bridge's shear modulus	I_{gc}	Bridge's momentum of torsion inertia
ρ_c	Bridge's mass density	H_p	Plate's Hamilton functional
H_{rb}	Rib's bending Hamilton functional	H_{rt}	Rib's torsion Hamilton functional
H_{bb}	Bridge's bending Hamilton functional	H_{bt}	Bridge's torsion Hamilton functional

Because of the small height of the rib compared to its width, torsional inertia doesn't take into account warping. Moreover, because of the plate controls the rib's motion, the action of the whole system is expressed as a function of transversal displacement of the plate and its spatial and temporal derivatives.

For a structure with a determined number N_r of ribs in the direction $\vec{y}$ and a bridge (stronger rib) in the direction $\vec{x}$, we express the entire functional by :

$$H_{Soundboard} = H_p + \sum_{i=1}^{N_r} \left(H_{rb}^{(i)} + H_{rt}^{(i)} \right) + H_{bb} + H_{bt} \tag{8}$$

2.3 Decomposition on the basis of simply supported unribbed plate's modes

We decompose the motion of the plate on the basis of simply supported plate's modes in order to write a generalized matrix problem. This basis is appropriated to an analytical approach and

currently used in the area of vibrations [10, 11]. The transversal displacement of the plate is written as a linear combination of unribbed plate's modes weighted by modal amplitudes $a_{mn}(t)$:

$$w(x,y,t) = \sum_{m=1}^{M} \sum_{n=1}^{N} a_{mn}(t)\phi_{mn}(x,y) \tag{9}$$

where $\phi_{mn}(x,y) = sin\left(\frac{m\pi}{l}x\right) sin\left(\frac{n\pi}{L}y\right)$.

We note that modal shapes of the simply supported (unribbed) plate are orthogonal that permits us to realize analytically the surface integral of the Hamilton functional.
In that case, the functional depends of the couple of variables ($a_{mn}(t)$,$\dot{a}_{mn}(t)$) and no more of the transversal displacement $w(x,y,t)$ and its space and temporal derivatives $w_{,x}$, $w_{,xx}$, $w_{,yy}$, $w_{,xy}$ and $\dot{w}$. So, we note :

$$H_{soundboard} = \int_{t_0}^{t_1} \mathcal{L}(a_{mn}(t), \dot{a}_{mn}(t))\, dt \tag{10}$$

where $\mathcal{L}(a_{mn}(t), \dot{a}_{mn}(t))$ is called Lagrangian of the system.

2.4 Matrix formulation

In analytical mechanics every vibrating system is governed by the principle of less action also named Hamilton's principle. In practice, we use the differential form of Euler-Lagrange to determine the evolution of the system. Let, the following equations :

$$\delta H_{soundboard} = 0 \Leftrightarrow \frac{\partial \mathcal{L}}{\partial a_{pq}} - \frac{d}{dt}\frac{\partial \mathcal{L}}{\partial \dot{a}_{pq}} = 0 \tag{11}$$

express for each mode of the unribbed plate and where $p = 1 \rightarrow M$ et $q = 1 \rightarrow N$.

This minimization combined with the orthogonal properties of the simply supported plate's modes leads us to a single equation for a particularly mode "pq".
We finally get a homogeneous problem for which the size is conditioned by the number of unribbed plate's modes taken into account needed for the convergence of the solution. Let:

$$\begin{array}{c} \left\{[M_p^{plate}] + [M_{pn}^{ribs} + [M_{pn}^{bridge}]\right\} \ \{\ddot{a}_p\} \\ + \left\{[K_p^{plate}] + [K_{pn}^{ribs} + [K_{pn}^{bridge}]\right\} \ \{a_p\} = \bar{0} \end{array} \tag{12}$$

where $p = (m,n)$ et $n = (r,s)$.

A matrix formulation permits efficient numerical calculus. Furthermore, expressing the problem by this way shows easily the coupling phenomena due to the presence of superstructures. Contrary to the matrices linked to the plate which are diagonal, those linked to the ribs are full and symmetric. So, superstructures introduce a coupling of unribbed plate's modes which is very strong as we will see in the following sections.
For a harmonic matter, the equation 12 becomes :

$$\left(\bar{\bar{K}} - \omega^2 \bar{\bar{M}}\right) \bar{a} = \bar{0} \tag{13}$$

where $\bar{\bar{K}}$ and $\bar{\bar{M}}$ are respectively rigidity and mass generalized matrix of the whole ribbed plate and $\bar{a}$ the vector of modal amplitudes $\bar{a}_{pq}$.

In the following results, we have increased step by step the number of unribbed plate's modes taken into account to stabilization of eigenfrequencies in high frequencies. It brings up approximately to order M and N of 40 and 30.

2.5 Eigenvalue problem

The research of eigenvalues and eigenvectors of the $\bar{\bar{M}}^{-1}\bar{\bar{K}}$ matrix solving equation 13 leads us to a diagonal matrix of eigen angular frequencies and to a matrix of eigenvectors. Each terms of eigenvectors are the modal amplitudes weighting the eigen modes of the unribbed plate used to re-create modes of ribbed plate (see equation 9). By this way, we determine the modal shapes of the ribbed structure.

Dimensions of the plate and superstructures are taken from [7] (cheap upright piano's soundboard). We note that ribs become less and less important when we go from right to left in the figure 2 (towards high keys). For this study, the frequency range of interest is [0;5000] Hz.
The presence of only one strong rib in the direction $\vec{x}$ (bridge) seems to separate the plate in two parts. We often find a vibrating area and a non-vibrating area in each side of this one (3^{th}, 4^{th} and 5^{th} mode in figure 3).

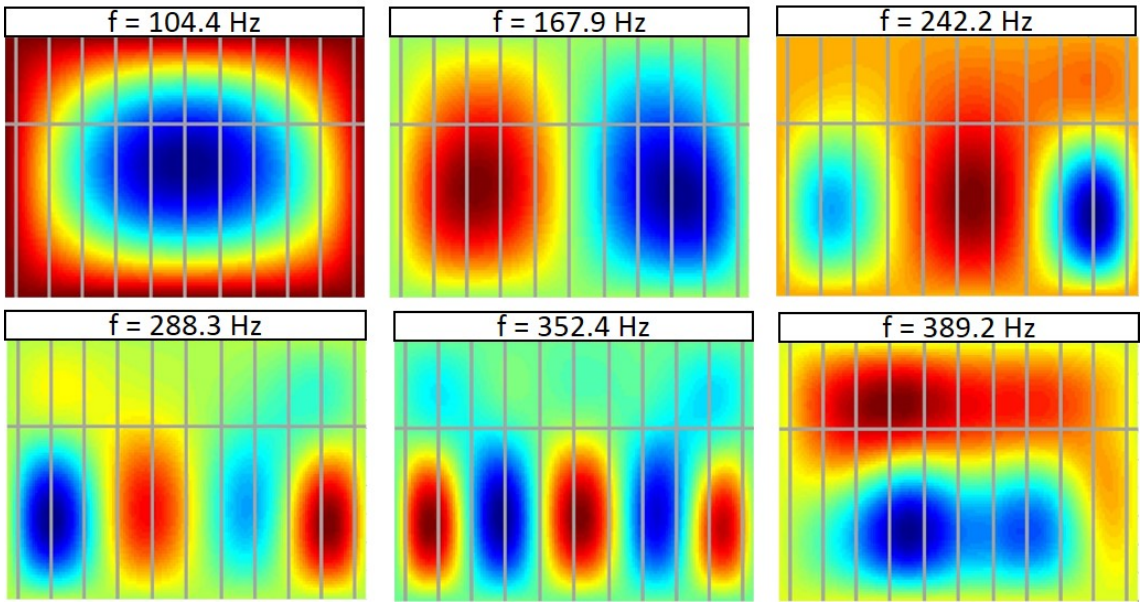

Figure 3. 1^{st} to 6^{th} modes of the ribbed plate.

In these conditions, only the first mode seems to be similar to an homogeneous unribbed plate's mode even if the second is not so far. The separating effect appears from the third mode (242 Hz) creating two virtual plates and in each of them, the vibration is approximately homogeneous. With this consideration, the ribbed structure appears like an equivalent homogeneous unribbed plate but only on a reduced area delimited by the bridge.
Several other authors [6–8] have shown through statistical indicator (modal density) that the piano soundboard in playing situation appears like an equivalent homogeneous unribbed plate under 800/1000 Hz.

A regular adding of ribs also implies phenomena of localizations in the inter-rib spaces. Authors in [7, 8] show that these localizations appear when the wavelength in the direction of the strong Young modulus (fiber of wood) becomes approximately equal to the inter-rib spaces (approximately at 800Hz). Even if our geometry is simplified, our calculus show that the majority of localizations appears in the conditions described by the aforementioned authors. The figure 4 presents one of these modes.

The method that we develop permits to calculate quickly high frequency modes. Figure 5

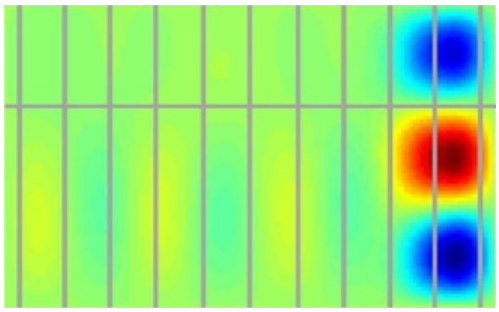

Figure 4: 11^{th} mode of the ribbed plate with a frequency of 610.9 Hz presenting a localization of the vibration in the inter-ribbed spaces.

presents one of these modes which highlights many vibrating phenomena with particularly oblique waves or localized wave's reflections between ribs.

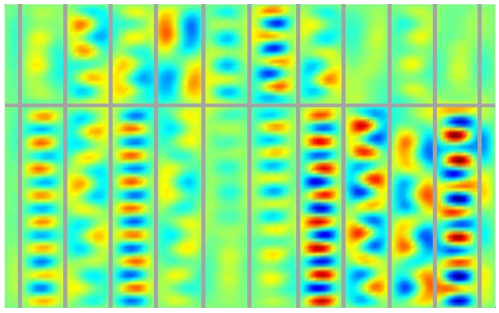

Figure 5: 288^{th} mode of the ribbed plate with a frequency of 4190 Hz presenting complex vibratory phenomena.

Finally, in order to re-create approximately the 350 modes of the ribbed plate in the frequency range [0;5000] Hz, we need around 1200 simply supported plate's modes that is to say modes with very small wavelengths.

3 ACOUSTIC RADIATION OF A RIBBED STRUCTURE

The piano soundboard's modeling developed here is not only limited to vibratory aspects but can also embrace its radiation. The structure is considered as baffled. We are interested more specifically in some general indicators as acoustical radiated power, space average velocity and radiation coefficient.

3.1 Forced response

In order to calculated the acoustic radiation of the structure, we first determine the forced response for a specific excitation. We consider a punctual excitation with an amplitude of one Newton. This external effort $F(x_e, y_e, t) = F\delta(x - x_e)\delta(y - y_e)e^{j\omega_e t}$ is harmonic, punctual and applied to the coordinates (x_e, y_e). We define the vector of generalized effort $\bar{F}_{gen}$ and these components are defined by the following relation :

$$F_{pq} = F\ \phi_{pq}(x_e, y_e) \tag{14}$$

So the formulation is the same that equation 13 but with a second member. The acoustical boundary pressure is actually ignored. So, the classical light fluid assumption is made to determine the

vibrational behavior of the structure. We calculate the vector of modal amplitudes for a particular excitation. Let :

$$\bar{a} = \left(\bar{\bar{K}} - \omega_e^2 \bar{\bar{M}}\right)^{-1} \bar{F}_{gen} \tag{15}$$

Structural damping is taken into account by making complex the rigidity matrix $\bar{\bar{K}}$. Ege *et al.* show in [7] that the structural damping measured on the upright soundboard made of spruce in playing situation varies between 1% and 3%. So, we have chosen to apply a constant coefficient of 2% for all the frequencies.

3.2 Expression of acoustical radiated power, space average velocity and radiation coefficient

The vibration of the structure is transmitted to the fluid and we are interested in the radiated power, space average velocity and radiation coefficient. The expression of the radiated power is well known and given in the literature [12] :

$$W(\omega) = \frac{\omega^2}{2} \sum_m \sum_n |a_{mn}(\omega)|^2 R_{mnmn}(\omega) \tag{16}$$

where a_{mn} are the modal amplitudes given by equation 15 and $R_{mnmn}(\omega)$ the real part of acoustical radiation impedance.
Moreover, this expression of the acoustical power supposes to ignore the acoustical intermodal coupling of the unribbed plate's modes. Obviously, the a_{mn} vector is obtained with the system 15 fully coupled where the strong mechanical cross modal coupling is taken into account.
$R_{mnmn}(\omega)$ are calculated numerically and given by the following expression :

$$R_{mnmn}(\omega) = \frac{\rho_0 \omega}{\pi^2} \int_0^k \int_0^k \frac{|\tilde{\phi}_{mn}(k_x, k_y)|^2}{\sqrt{k^2 - k_x^2 - k_y^2}} \, dk_x \, dk_y \tag{17}$$

where $\tilde{\phi}_{mn}(k_x, k_y) = \int_0^l \int_0^L e^{-jk_x x} e^{-jk_y y} \phi_{mn}(x, y) \, dx \, dy = \frac{1-(-1)^m e^{-jk_x l}}{\left(\frac{m\pi}{l}\right)^2 - k_x^2} * \frac{1-(-1)^n e^{-jk_y L}}{\left(\frac{n\pi}{L}\right)^2 - k_y^2}$.

The space average velocity is defined as :

$$< v^2 > (\omega) = \frac{1}{2S} \int_S |v(x, y, \omega)^2| \, dS = \frac{\omega^2}{8} \sum_m \sum_n |a_{mn}(\omega)|^2 \tag{18}$$

where S is the surface of the plate.

To finish, the radiation coefficient is defined as :

$$\sigma(\omega) = \frac{1}{\rho_0 c S} \frac{W(\omega)}{< v^2 > (\omega)} \tag{19}$$

where ρ_0 and c are respectively the mass density and the velocity of sound in the air.

3.3 Numerical applications

3.3.1 Influence of the excitation point

In this section we will study the influence of the excitation point on the same structure that before (simplified soundboard). These three points (see figure 6) are all at the abscissa $x_e = 1$m and at the ordinate :

- $y_e = 0.61$m in black, on the most important superstructure (bridge),
- $y_e = 0.56$m in red, on the plate near the last one,
- $y_e = 0.47$m in green, on the plate far of the first points, near the middle between the edge of the plate and the bridge.

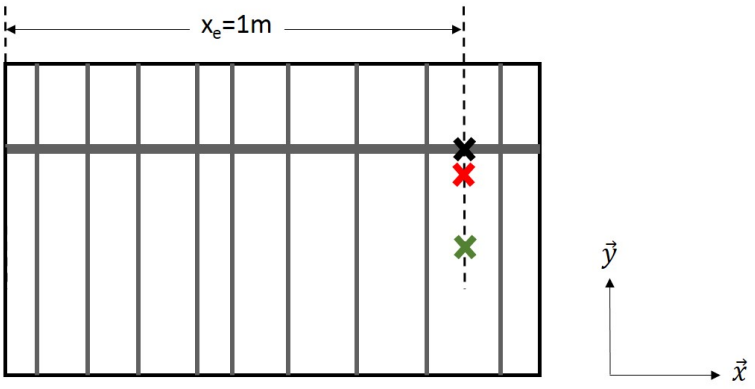

Figure 6. Drawing of the positions of the three excitation points.

Before that, let's define the critical frequency f_c of a plate. At this frequency, the propagation's velocity of flexural waves in the plate and in the fluid (air) are the same. Below this frequency the bending wave is subsonic and poorly radiative, higher it is supersonic and radiative.
For a simple case like an unribbed isotropic plate, we can determine easily the propagation's velocity of the flexural wave in the structure. So, we have the following expression of the critical frequency for an isotropic plate :

$$f_c = \frac{c^2}{2\pi h}\sqrt{\frac{12\rho(1-\nu^2)}{E}} \tag{20}$$

depending on the velocity of propagation of the wave in the fluid c, the plate's thickness h, the plate's mass density ρ, the Young modulus E and the Poisson's coefficient ν of the plate.

For an orthotropic plate, there are two critical frequencies because of different propagation's velocities due to the two Young modulus. In our case, these frequencies are around 1450 Hz and 7250 Hz. For a structure with complex geometry and superstructures, it's impossible to calculate f_c and has no more sens. Nevertheless, we define the apparent critical frequency when the radiation coefficient becomes around unity (0 dB in log scale).

In this way, the apparent critical frequency is lower than 1450 Hz for our three cases. As shown in figure 7-c, higher than 800 Hz (zone III and IV) every alerted modes are radiative ; on the contrary at low frequencies (zone I), the modes are poorly radiative and this, independently of the excitation point.
A transitional frequency range can be defined where the excitation position has an influence on the radiation efficiency (zone II). So, exciting on a hard point of the structure (or close to it) tends to increase the radiation factor in this transitional range : the apparent critical frequency decreases from 800 Hz (green plot) to 400 Hz (black and red plots). Far from the bridge, the radiation factor is poor in zone II.

However, the influence of the excitation point on the acoustical radiated power and the space average velocity is different (figures 7-a and 7-b). Indeed, in high frequencies (zone IV), the behavior when both excitations are placed directly on the plate are similar (red and green plots) ;

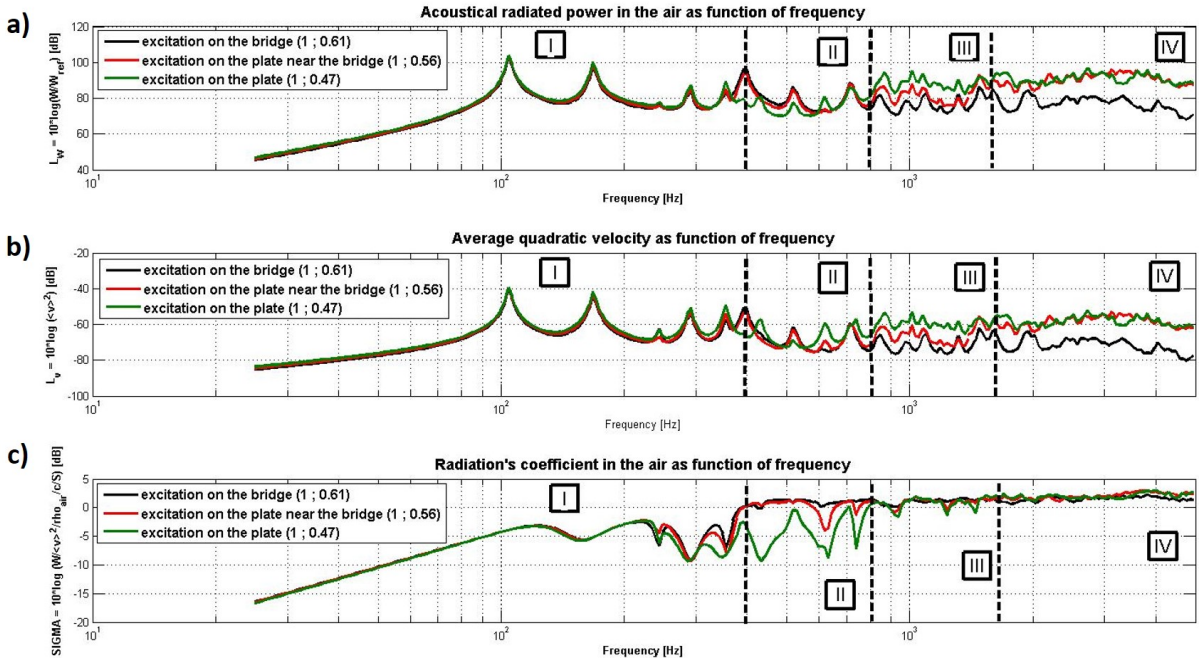

Figure 7: Radiated power, space average velocity and radiation coefficient as functions of frequency for three different excitation points.

when the excitation is exactly on the bridge (black plot), the response is 15 dB lower. Obviously, the bridge has a lower mobility and that's why an excitation on the hardest point of this heterogeneous structure leads to decrease the radiated power as well as the average plate's velocity.
On the contrary, in zone I and II (low frequencies) the excitation point has less influence on these parameters. These results show also a transitional behavior between the three cases in zone III. Contrary to excitations on a "hard" point (lowest mobility in black) and on a "weak" point (highest mobility in green), for an excitation point close to the bridge (red plot) the acoustical radiated power as well as the average velocity are between the two other curves in the frequency range [800;1500] Hz.

Finally, these results show that an excitation on a hard point implies a decreasing of the average velocity and of the acoustical radiated power in favor of a better radiation efficiency in mid frequency.
From a musical point of view, strings are traditionally attached to the bridge due to practical reasons. Our results show that a smaller bridge could increase the acoustical power in high pitched notes but it also implies an increasing of the mobility of this one and so a lower sustain.
It raises the question of the optimal dimensions of the bridge in order to find the best acoustical power/sustain trade-off.

3.3.2 Influence of the ribs

Let study now the influence of the ribs on the radiation. For that, we keep the excitation applied on the strong superstructure (bridge) and choose two different ribbed structures (see figure 8) : ribbed in two directions (simplified soundboard) and the same without ribs in the direction $\vec{y}$.

Note that in the case of piano soundboard, ribs have mainly a static effect: they balance the weakness of wood in the perpendicular direction of fibers (fibers are parallel to the bridge in the direction $\vec{x}$). So, the simple removal of ribs in the direction $\vec{y}$ implies an important loss of rigidity

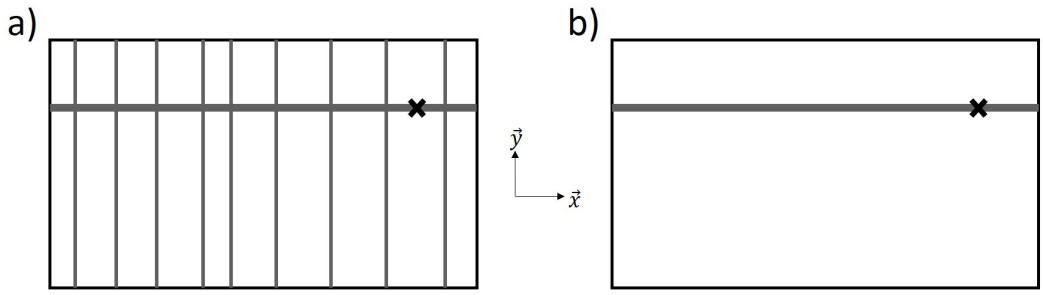

Figure 8: Drawing of two ribbed structures. (a) : simplified soundboard. ; (b) : soundboard without ribs.

in the same direction.
That's why we also consider a third case based on the same geometry. We create an equivalent soundboard with an equivalent rigidity. For that, we increase the Young modulus in the weak direction $\vec{y}$ in order to equalize the first eigenfrequency of unribbed (blue plot in figure 9) and ribbed structure (black plot in figure 9). It leads us to a new Young modulus $E_{y\ new} \approx 3.33 * E_x$, showing a strong overcompensation of orthotropy. The other features of the plate (width, length, height, mass density) are not changed.

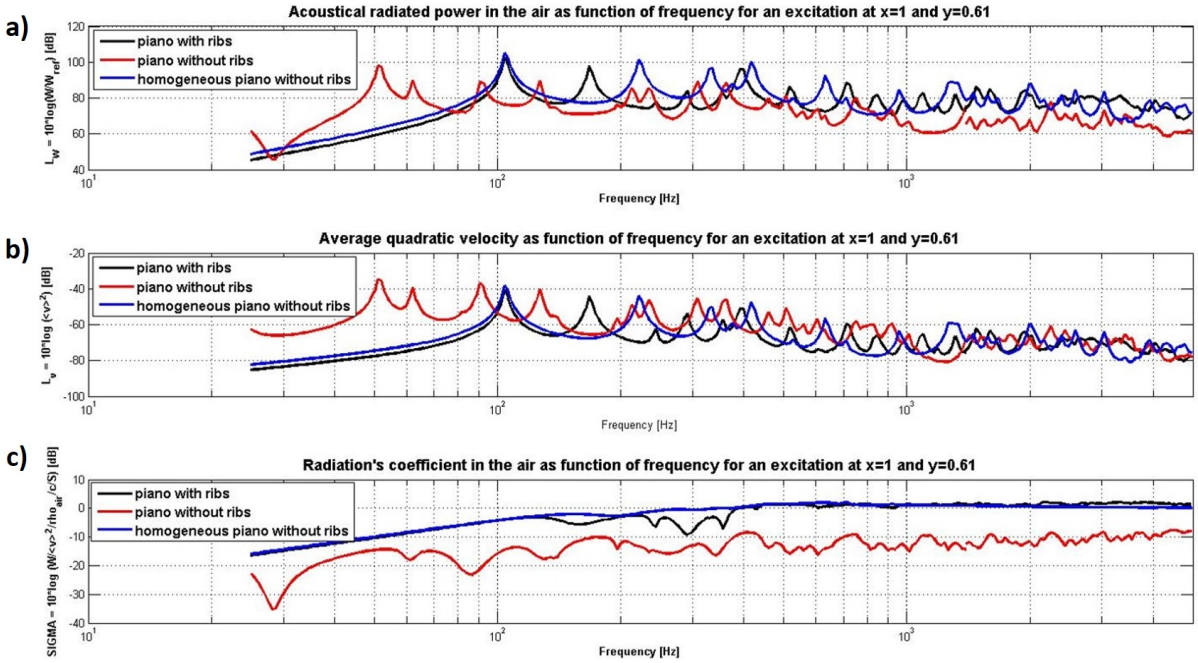

Figure 9: Radiated power, space average velocity and radiation coefficient as functions of frequency for the simplified soundboard, the one without ribs and the homogeneous panel (excitation on the bridge).

Due to the important loss of rigidity, first eigenfrequencies are lower than in the other case when we remove ribs (red plot in figure 9-a and b). It implies an increase of radiation in low frequencies due to an increase of velocity, the structure becoming very flexible. This flexible effect is obvious at low and mid frequency where the velocity is more important than the reference case (black plot) but beyond that, the velocity tends to the same value. The loss of rigidity also move the apparent critical frequency of the unribbed plate higher than 5000 Hz(figure 9-c). In that case, the efficiency of the radiation is really bad and the radiated power weak. It shows the utilities of the rigidity brought by the ribs on the piano soundboard's radiation from an acoustical point of view and not

only a static point of view.

In the other hand, the ribs create complex modal shapes which relatively have bad radiation coefficients in the frequency range [150;400] Hz as showing by the radiation coefficients' comparison between black plot (piano with ribs) and blue plot (homogenize piano) in figure 9-c. Indeed, we can see globally that the velocities have the same average values that is logical because the global rigidities are equal. But we see that in this frequency range, the radiation coefficient is better when the plate is homogenize. So the alerted modes produce more power for the same velocity, implying a better radiated power.
At low and high frequencies, this modification has no influence on the average values of each indicators (blue and black plots on figure 9-a, b and c).

4 CONCLUSION

This article has presented the basis of a new analytical modeling method for the vibrations and the radiations of orthotropic ribbed plates with complex geometry and shows that an homogeneous plate with a bridge could increase the radiation efficiency in mid frequency with few modifications of the acoustical power. In this paper, we have limited our study to the case of a rectangular special orthotropic plate with ribs in two perpendicular directions but we are actually able to describe a complex geometry [13] (non-rectangular plate or plate with an angle of orthotropy for example). Results are encouraging and in a good agreement with published results especially impedances at the bridge and far from the bridge but also eigenmodes and vibratory responses at typical frequency [14].
In order to validate the presented analytical numerical method, measurements will take place soon in the few months and finite element modeling will be done.

ACKNOWLEDGMENTS

This work was performed within the framework of the Labex CeLyA of Universit de Lyon, operated by the French National Research Agency (ANR-10-LABX-0060/ ANR-11-IDEX-0007).

REFERENCES

[1] I. Brémaud. *Diversité des bois utilisés ou utilisables en facture d'instruments de musique*. PhD thesis, Université Montpellier II, 2006.

[2] I. Brémaud and N. Poidevin. *Approches culturelles et mécaniques dans le choix des bois en facture: cas des archets anciens*. 5th Conference on Interdisciplinary Musicology (Paris), 2009.

[3] H. Suzuki. Acoustics of pianos. *Applied Acoustics*, 30(2):147–205, 1990.

[4] H. A. Conklin. Design and tone in the mechanoacoustic piano. part ii. piano structure. *J. Acoust. Soc. Am.*, 100(2):695–708, 1996.

[5] N. Giordano. Mechanical impedance of a piano soundboard. *J. Acoust. Soc. Am.*, 104(4):2128–2133, 1998.

[6] J. Berthaut, M. N. Ichchou, and L. Jezequel. Piano soundboard : structural behavior, numerical and experimental study in the modal range. *Applied Acoustics*, 64(1):1113–1136, 2003.

[7] K. Ege, X. Boutillon, and M. Rébillat. Vibroacoustics of the piano soundboard : (non)linearity and modal properties in the low- and mid-frequency ranges. *Journal of Sound and Vibration*, 332(5):1288–1305, 2013.

[8] X. Boutillon and K. Ege. Vibroacoustics of the piano soundboard : Reduced models, mobility synthesis, and acoustical radiation regime. *Journal of Sound and Vibration*, 332(18):4261–4279, 2013.

[9] A. Chaigne, B. Cotté, and R. Viggiano. Dynamical properties of piano soundboards. *J. Acoust. Soc. Am.*, 133(4):2456–2466, 2013.

[10] B. Laulagnet and J. L. Guyader. Sound radiation by finite cylindrical ring stiffened shells. *Journal of Sound and Vibration*, 138(2):173–191, 1990.

[11] B. Laulagnet and J. L. Guyader. Structural acoustic radiation prediction : expanding the vibratory response on a functional basis. *Applied Acoustics*, 43(3):247–269, 1994.

[12] C. Lesueur. *Rayonnement acoustique des structures : vibroacoustique, interactions fluide-structure*. Collection de la Direction des tudes et recherches d'Electricit de France. Ed. Eyrolles (Paris, France), Paris, 1988.

[13] B. Trévisan, K. Ege, and B. Laulagnet. *Prediction of orthotropic ribbed plates' vibro-acoustics mechanisms : application to the piano soundboard*. International Symposium on Musical Acoustics (Mans, France), 2014.

[14] B. Trévisan, K. Ege, and B. Laulagnet. *Développement d'une méthode analytique pour la prédiction des mécansimes vibro-acoustiques des plaques orthotropes raidies de formes quelconques : application la table d'harmonie de piano*. Congrès Français d'Acoustique (Poitiers, France), 2014.